JACS
JOURNAL OF THE AMERICAN CHEMICAL SOCIETY

Communication

pubs.acs.org/JACS

Construction of Covalent Organic Frameworks Bearing Three Different Kinds of Pores through the Heterostructural Mixed Linker Strategy

Zhong-Fu Pang, Shun-Qi Xu, Tian-You Zhou, Rong-Ran Liang, Tian-Guang Zhan, and Xin Zhao*

Key Laboratory of Synthetic and Self-Assembly Chemistry for Organic Functional Molecules, Shanghai Institute of Organic Chemistry, Chinese Academy of Sciences, 345 Lingling Road, Shanghai 200032, China

Supporting Information

ABSTRACT: It is very important to create novel topologies and improve structural complexity for covalent organic frameworks (COFs) that might lead to unprecedented properties and applications. Despite the progress achieved over the past decade, the structural diversity and complexity of COFs are quite limited. In this Communication, we report the construction of COFs bearing three different kinds of pores through the heterostructural mixed linker strategy involving the condensation of a D_{2h}-symmetric tetraamine and two C_2-symmetric dialdehydes of different lengths. The complicated structures of the triple-pore COFs have been confirmed by powder X-ray diffraction and pore size distribution analyses.

Covalent organic frameworks (COFs) have become a prominent field of research since their discovery in 2005.[1] As an emerging class of crystalline porous materials, COFs exhibit great potential applications in various fields, including gas storage,[2] separation,[3] catalysis,[4] energy storage,[5] and photoelectric devices.[6] It is generally accepted that the topology of a COF has a significant influence on its properties. Although a variety of COFs have been synthesized over the past decade,[7] compared to their analogues, metal−organic frameworks (MOFs),[8] the topology and complexity of COFs are quite limited. The abundant and highly complicated topologies of MOFs can be attributed not only to the diversity of building blocks but also to the flexible approaches to their assembly. Among those approaches, the mixing of blocks with different structures, known as the heterostructural mixed linker approach, enables the construction of MOFs with complicated structures from relatively simple building blocks.[9] We envisioned that this approach might also be a powerful tool to create novel topologies and improve structural complexity for COFs. However, to date, whether the heterostructural mixed linker approach is applicable to the construction of COFs have never been demonstrated. To examine this possibility, in this work, we chose a dual-pore (DP) COF, which bears two different kinds of pores previously reported by us, as a model system.[10] The DP-COF, denoted as **COF-TPA**, was prepared from the condensation of 4,4′,4″,4‴-(ethene-1, 1,2,2-tetrayl)tetraaniline (**ETTA**) with terephthaldehyde (**TPA**). To achieve the mixing of linkers, two longer dialdehydes, [1,1′-biphenyl]-4,4′-dicarbaldehyde (**BPDA**) and [1,1′:4′,1″-terphenyl]-4,4″-dicarbaldehyde (**TPDA**), were selected. These two dialdehydes, together with **TPA**, constitute a linker pool from which we can choose two to copolymerize with **ETTA**. For the copolymerization reaction, there are several possibilities. First, it might yield amorphous polymers, as a result of mutual interference of the different linkers. Second, two kinds of dual-pore COFs might be generated simultaneously through self-sorting of the linkers. Third, if the heterostructural mixed linker approach works for COFs, there will be no self-sorting, but both linkers will integrate to afford a new COF whose topology is totally different from those of the COFs prepared from the condensation of **ETTA** with either of the two dialdehydes. We herein report the construction of unprecedentedly complicated COFs which bear three different kinds of pores through the condensation of **ETTA** and two different dialdehydes. Moreover, two dual-pore COFs were also synthesized for comparison (Scheme 1). These results indicate that the heterostructural mixed linker approach has a great potential to fabricate COFs with higher hierarchy and complexity.

This proof-of-concept study was carried out in two steps. First, COFs were assembled from the condensation reaction of **ETTA** with **BPDA** or **TPDA**. Second, three-component condensation reactions were performed using **ETTA**, **TPA**, and **BPDA** or **ETTA**, **BPDA**, and **TPDA**. All the reactions were carried out under solvothermal condition (see Supporting Information for details). The as-obtained yellow powders were denoted as **COF-BPDA** (from **ETTA** and **BPDA**), **COF-TPDA** (from **ETTA** and **TPDA**), **SIOC-COF-1** (from **ETTA**, **TPA**, and **BPDA**), and **SIOC-COF-2** (from **ETTA**, **BPDA**, and **TPDA**), respectively.

Elemental analyses of these powders revealed that their C, H, and N contents were very close to the corresponding theoretical values calculated from the expected polymerization products (see Supporting Information for details). The carbon contents of these polymers increased along with the increasing number of benzene ring in the polymers, which was also consistent with the theoretical prediction. The Fourier transform infrared (FT-IR) spectra of the COFs show the stretching band of C═N at 1619.8 cm^{-1}, confirming the formation of imine linkages in the polymers (Figure S1). The characteristic resonance peaks of imine carbons (around 157 ppm) were observed in solid-state ^{13}C cross-polarization/magic angle spinning nuclear magnetic resonance (CP/MAS NMR) spectra of the COFs, again confirming the existence of imine linkages (Figures S2−S5). Thermogravimetric analyses (TGA) indicated that the as-obtained polymers were

Received: February 3, 2016
Published: March 25, 2016

DOI: 10.1021/jacs.6b01244
J. Am. Chem. Soc. 2016, 138, 4710−4713

Scheme 1. Cartoon Representation for the Synthesis of Dual-Pore and Triple-Pore COFs

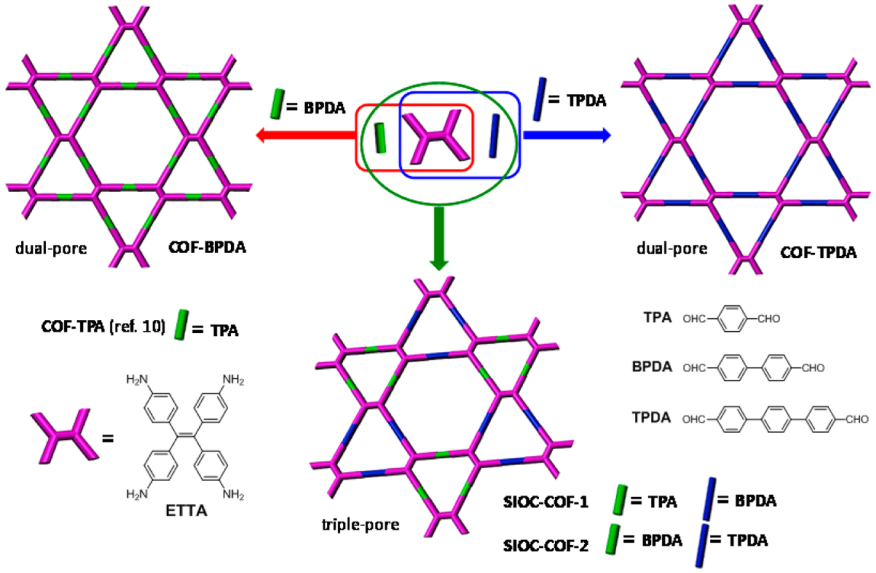

highly thermostable. Less than 4% weight loss was observed for these materials when the temperature increased from 25 to 450 °C (Figure S6). Scanning electron microscopy (SEM) revealed that they all exhibited irregular morphology (Figure S7).

To determine the crystal structures of the as-obtained polymers, theoretical simulations and powder X-ray diffraction (PXRD) experiments were conducted. The simulations were carried out by using Materials Studio version 7.0. Similar to the dual-pore COF reported before,[10] two types of possible 2D structures were generated for **COF-BPDA** and **COF-TPDA**, that is, dual-pore structures and single-pore (SP) structures. For each type of the structures, eclipsed stacking (AA) and staggered stacking (AB) were constructed (Tables S1 and S2). In the experimental PXRD profile of **COF-BPDA** (Figure 1a, black

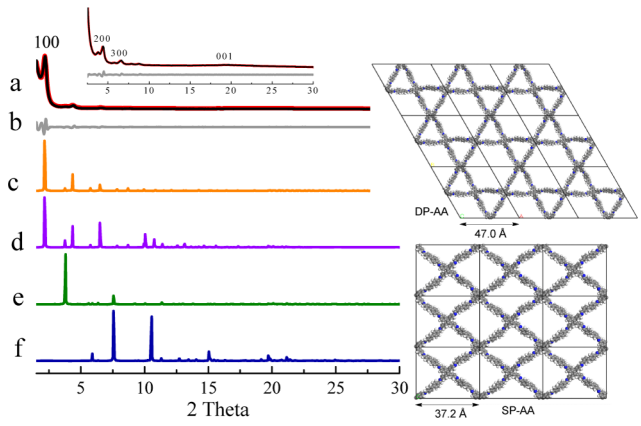

Figure 1. (a) Experimental (black) and refined (red) PXRD patterns of **COF-BPDA**, (b) difference plot between the experimental and refined PXRD patterns, and simulated PXRD patterns of **BPDA**-based (c) DP-AA, (d) DP-AB, (e) SP-AA, and (f) SP-AB structures.

curve), a strong peak at 2.19° together with some relatively weaker peaks at 3.82°, 4.41°, 6.65°, and ca. 19.4° were observed, which were assigned to (100), (110), (200), (300), and (001) diffractions. This PXRD pattern was in good agreement with the simulated PXRD pattern of **BPDA**-based DP-AA structure (Figures 1c and S8), which strongly suggests that **COF-BPDA** holds a dual-pore structure with AA stacking model. Subsequently, Pawley refinement yielded unit cell parameters of $a = b = 46.83$ Å, $c = 4.50$ Å, $\alpha = \beta = 90°$, and $\gamma = 120°$, with factors of $R_P = 2.96\%$ and $R_{WP} = 3.67\%$. The refined PXRD pattern well reproduced the experimental PXRD pattern, as revealed by the difference plot (Figure 1b). In the case of **COF-TPDA**, diffraction peaks corresponding to the reflections from (100), (110), (200), (210), (300), (220), (400), and (001) planes were observed at 1.86°, 3.27°, 3.75°, 4.99°, 5.62°, 6.68°, 7.50° and ca. 19.7°, respectively (Figure S9), on the basis of which a dual-pore structure with AA packing was assigned for it, after the comparison with the simulated PXRD pattern. Pawley refinement yielded unit cell parameters of $a = b = 55.29$ Å, $c = 4.50$ Å, $\alpha = \beta = 90°$, and $\gamma = 120°$, with factors of $R_P = 3.58\%$ and $R_{WP} = 5.34\%$, which matched with the experimental data quite well.

After the structures of the two dual-pore COFs were established, the validity of constructing COFs through heterostructural linker strategy was examined. The as-prepared powders **SIOC-COF-1** and **SIOC-COF-2** were also subjected to PXRD analyses. In the case of **SIOC-COF-1**, a strong peak at 2.42° (100) was observed (Figures 2 and S10). This peak neither

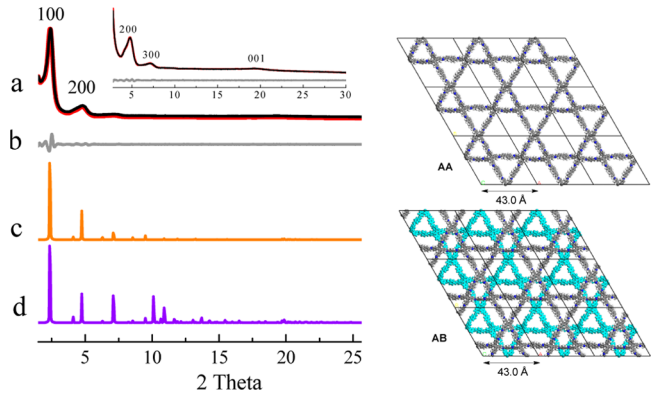

Figure 2. (a) Experimental (black) and refined (red) PXRD patterns of **SIOC-COF-1**, (b) difference plot between the experimental and refined PXRD patterns, and simulated PXRD patterns of triple-pore COF with (c) AA and (d) AB stacking.

DOI: 10.1021/jacs.6b01244
J. Am. Chem. Soc. 2016, 138, 4710−4713

belonged to the (100) diffraction of **COF-BPDA** (2.19°) nor corresponded to the (100) diffraction of **COF-TPA** (2.78°), as clearly revealed by the comparison of the positions of the peaks (Figure S11). This result indicated the formation of a COF with new structure. In addition to the peak at 2.42°, a set of diffraction peaks which were assigned to (200), (300), and (001) planes were also observed at 4.81°, 7.15°, and ca. 19.4°, respectively. Since **SIOC-COF-1** was obtained by the condensation of **ETTA**, **TPA** and **BPDA** in a molar ratio of 1:1:1, a triple-pore (TP) COF in which half of the phenyl linkers in the dual-pore COF **COF-TPA** were replaced by biphenyl linkers was proposed and constructed. It generated a COF whose unit consists of an inequilateral hexagon, three phenyl-based small triangles and three biphenyl-based big triangles (see Scheme 1 for its structure). Theoretical simulation was performed for this triple-pore COF, which generated unit cell parameters of $a = b = 43.0$ Å, $c = 4.5$ Å (AA stacking) or 9.0 Å (AB stacking), $\alpha = \beta = 90°$, and $\gamma = 120°$ (Table S3). The simulated PXRD pattern generated from triple-pore structure with AA stacking was in good agreement with the experimentally observed PXRD pattern of **SIOC-COF-1**, suggesting it holds a structure with three different kinds of pores and AA stacking model. Pawley refinement reproduced the experimental PXRD pattern quiet well and yielded unit cell parameters of $a = b = 42.63$ Å, $c = 4.50$ Å, $\alpha = \beta = 90°$, and $\gamma = 120°$, with factors of $R_P = 2.59\%$ and $R_{WP} = 3.31\%$.

For **SIOC-COF-2** which was prepared from the condensation of **ETTA**, **BPDA**, and **TPDA**, a set of diffraction peaks at 1.96°, 3.88°, 5.84°, and ca. 19.7° ,assignable to (100), (200), (300), and (001) planes were observed in its experimental PXRD pattern (Figures 3 and S12). This set of peaks was totally different from

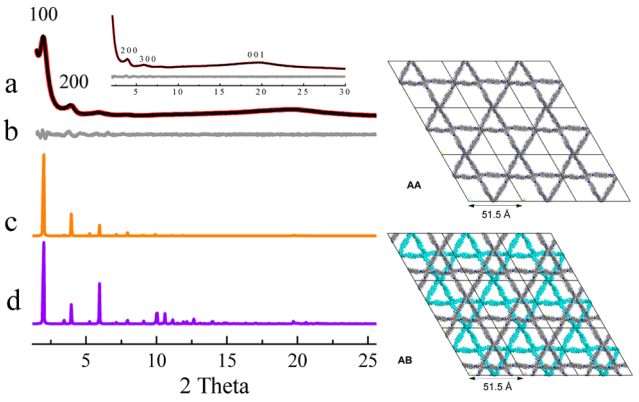

Figure 3. (a) Experimental (black) and refined (red) PXRD patterns of **SIOC-COF-2**, (b) difference plot between the experimental and refined PXRD patterns, and simulated PXRD patterns of triple-pore COF with (c) AA and (d) AB stacking.

that of **COF-BPDA** and **COF-TPDA** (see Figure S13 for the comparison), indicating a new COF was obtained. A triple-pore structure similar to **SIOC-COF-1** was theoretically constructed, and the simulation gave unit cell parameters of $a = b = 51.5$ Å, $c = 4.5$ Å (AA stacking) or 9.0 Å (AB stacking), $\alpha = \beta = 90°$, and $\gamma = 120°$. The simulated PXRD pattern of a triple-pore COF with AA stacking well matched with the experimentally observed PXRD pattern of **SIOC-COF-2**. Pawley refinement produced unit cell parameters of $a = b = 51.42$ Å, $c = 4.49$ Å, $\alpha = \beta = 90°$, and $\gamma = 120°$, with factors of $R_P = 1.53\%$ and $R_{WP} = 2.04\%$. This result confirmed again that triple-pore COF could be produced from the three-component condensation. It should be noted that COFs which bear only one kind of pores may also be expected from the three-component condensation of the monomers used above. However, the formation of such structures was ruled out by the comparisons of the experimental PXRD patterns of the as-prepared materials with the simulated PXRD patterns of single-pore COFs (Figures S14 and S15).

To further corroborate the assigned crystal structures of the as-prepared COFs, nitrogen sorption measurements were carried out to assess their porosities and to analyze their pore size distributions (Figure 4). **COF-BPDA** and **COF-TPDA** exhibited

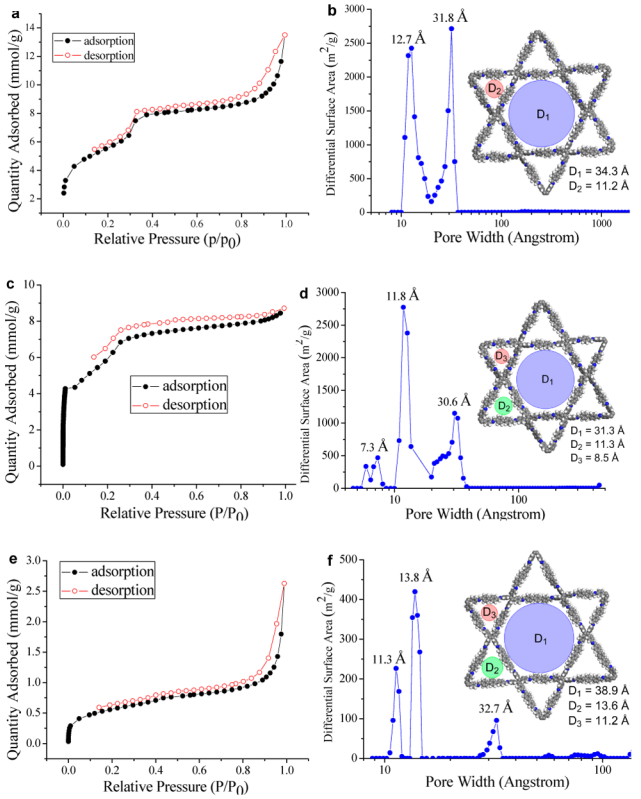

Figure 4. N_2 adsorption–desorption isotherms (77 K) of (a) **COF-BPDA**, (c) **SIOC-COF-1**, and (e) **SIOC-COF-2**, and pore size distribution profiles of (b) **COF-BPDA**, (d) **SIOC-COF-1**, and (f) **SIOC-COF-2**.

similar nitrogen sorption isotherms (Figure S16). The curves displayed a combination of type I and type IV nitrogen sorption isotherms,[11] suggesting that micropores and mesopores coexist in these two COFs. The BET surface areas calculated from the isotherms of **COF-BPDA** and **COF-TPDA** in the range of P/P_0 between 0.05 and 0.2 were 447.76 and 83.77 m^2/g for **COF-BPDA** and **COF-TPDA**, respectively (Figures S17 and S18). The total pore volumes (evaluated at $P/P_0 = 0.99$) of **COF-BPDA** and **COF-TPDA** were estimated to be 0.47 and 0.10 cm^3/g, respectively. The pore size distribution of **COF-BPDA** was generated by using nonlocal density functional theory (NLDFT), which revealed two main distributions at 12.7 and 31.8 Å (Figure 4b), indicating the existence of two kinds of pores of different sizes in the COF. The experimental pore size distributions are close to the theoretical pore sizes of **COF-BPDA** (11.2 and 34.3 Å as estimated by PM3 calculations), confirming again that **COF-BPDA** holds a dual-pore structure. Similarly, the pore size distribution analysis of **COF-TPDA** exhibits two main distributions at 14.8 and 37.0 Å, which is close

DOI: 10.1021/jacs.6b01244
J. Am. Chem. Soc. 2016, 138, 4710–4713

to its theoretical pore sizes (14.0 and 42.1 Å), indicating that **COF-TPDA** also possesses a dual-pore structure.

SIOC-COF-1 displayed a N_2 sorption isotherm similar to the above dual-pore COFs (Figure 4c). On the basis of its N_2 sorption data, BET surface area of **SIOC-COF-1** was calculated to be 478.41 m^2/g (Figure S19), and its total pore volume (evaluated at $P/P_0 = 0.99$) was estimated to be 0.30 cm^3/g. Pore size distribution analysis was performed for **SIOC-COF-1**. Three major pores around 7.3, 11.8, and 30.6 Å were observed (Figure 4d), which well matched with the theoretical pore sizes of the proposed triple-pore COF (8.5, 11.3, and 31.3 Å, as estimated by PM3 calculations). For **SIOC-COF-2**, BET surface area of 46.13 m^2/g (Figure S20) and total pore volume (evaluated at $P/P_0 = 0.99$) of 0.09 cm^3/g were obtained from its nitrogen sorption isotherm. Pore size distribution analysis revealed three main distributions around 11.3, 13.8, and 32.7 Å (Figure 4f). These values are consistent with the simulated pore distributions which were predicted to be 11.2, 13.6, and 38.9 Å. The results from pore size distribution analyses, together with the PXRD investigation, corroborated the obtention of triple-pore COFs from the three-component copolymerization. It should be noted that BET surface areas of **TPDA**-based COFs are quite low and the reason is currently unclear. However, it detracts nothing from the determinations of the crystal structures of the COFs.

In conclusion, COFs which bear three different kinds of ordered pores with controllable sizes have been constructed through the heterostructural mixed linker strategy. While the condensation of a D_{2h}-symmetric tetraamine and a C_2-symmetric dialdehyde gave rise to a dual-pore COF containing two different kinds of pores (triangular micropores and hexagonal mesopores), the copolymerization of a D_{2h}-symmetric tetraamine and two C_2-symmetric dialdehydes of different lengths produced a triple-pore COF in the unit of which an inequilateral hexagonal mesopore is alternatingly surrounded by three small triangular micropores and three big triangular micropores. These COFs represent a new topology with unprecedented hierarchy and structural complexity. This work for the first time demonstrates that the heterostructural mixed linker strategy can also be applicable to construction of COFs. It may open up a new way to fabricate COFs with sophisticated topologies from relatively simple building blocks. Its potential to construct more complicated COFs is currently under investigation in our laboratory.

■ ASSOCIATED CONTENT

Supporting Information

The Supporting Information is available free of charge on the ACS Publications website at DOI: 10.1021/jacs.6b01244.

Procedure for the preparation of the polymers, FT-IR spectra, solid-state ^{13}C CP-MAS NMR spectra, BET plots, TGA traces, and SEM images, including Figures S1−S20 and Tables S1−S8 (PDF)

■ AUTHOR INFORMATION

Corresponding Author

*xzhao@sioc.ac.cn

Notes

The authors declare no competing financial interest.

■ ACKNOWLEDGMENTS

We thank the National Natural Science Foundation of China (Nos. 21172249, 21472225) for financial support.

■ REFERENCES

(1) Côté, A. P.; Benin, A. I.; Ockwig, N. W.; O'Keeffe, M.; Matzger, A. J.; Yaghi, O. M. *Science* **2005**, *310*, 1166.

(2) (a) Han, S. S.; Furukawa, H.; Yaghi, O. M.; Goddard, W. A. *J. Am. Chem. Soc.* **2008**, *130*, 11580. (b) Doonan, C. J.; Tranchemontagne, D. J.; Glover, T. G.; Hunt, J. R.; Yaghi, O. M. *Nat. Chem.* **2010**, *2*, 235. (c) Rabbani, M. G.; Sekizkardes, A. K.; Kahveci, Z.; Reich, T. E.; Ding, R.; El-Kaderi, H. M. *Chem. - Eur. J.* **2013**, *19*, 3324. (d) Zeng, Y.; Zou, R.; Luo, Z.; Zhang, H.; Yao, X.; Ma, X.; Zou, R.; Zhao, Y. *J. Am. Chem. Soc.* **2015**, *137*, 1020.

(3) (a) Oh, H.; Kalidindi, S. B.; Um, Y.; Bureekaew, S.; Schmid, R.; Fischer, R. A.; Hirscher, M. *Angew. Chem., Int. Ed.* **2013**, *52*, 13219. (b) Ma, H.; Ren, H.; Meng, S.; Yan, Z.; Zhao, H.; Sun, F.; Zhu, G. *Chem. Commun.* **2013**, *49*, 9773.

(4) (a) Ding, S.-Y.; Gao, J.; Wang, Q.; Zhang, Y.; Song, W.-G.; Su, C.-Y.; Wang, W. *J. Am. Chem. Soc.* **2011**, *133*, 19816. (b) Fang, Q.; Gu, S.; Zheng, J.; Zhuang, Z.; Qiu, S.; Yan, Y. *Angew. Chem., Int. Ed.* **2014**, *53*, 2878. (c) Thote, J.; Aiyappa, H. B.; Deshpande, A.; Díaz Díaz, D.; Kurungot, S.; Banerjee, R. *Chem. - Eur. J.* **2014**, *20*, 15961. (d) Shinde, D. B.; Kandambeth, S.; Pachfule, P.; Kumar, R. R.; Banerjee, R. *Chem. Commun.* **2015**, *51*, 310. (e) Lin, S.; Diercks, C. S.; Zhang, Y.-B.; Kornienko, N.; Nichols, E. M.; Zhao, Y.; Paris, A. R.; Kim, D.; Yang, P.; Yaghi, O. M.; Chang, C. J. *Science* **2015**, *349*, 1208.

(5) (a) Deblase, C. R.; Silberstein, K. E.; Truong, T.-T.; Abruña; Dichtel, W. R. *J. Am. Chem. Soc.* **2013**, *135*, 16821. (b) DeBlase, C. R.; Hernández-Burgos, K.; Silberstein, K. E.; Rodríguez-Calero, G. G.; Bisbey, R. P.; Abruña, H. D.; Dichtel, W. R. *ACS Nano* **2015**, *9*, 3178. (c) Xu, F.; Xu, H.; Chen, X.; Wu, D.; Wu, Y.; Liu, H.; Gu, C.; Fu, R.; Jiang, D. *Angew. Chem., Int. Ed.* **2015**, *54*, 6814.

(6) (a) Wan, S.; Guo, J.; Kim, J.; Ihee, H.; Jiang, D. *Angew. Chem., Int. Ed.* **2008**, *47*, 8826. (b) Dogru, M.; Handloser, M.; Auras, F.; Kunz, T.; Medina, D.; Hartschuh, A.; Knochel, P.; Bein, T. *Angew. Chem., Int. Ed.* **2013**, *52*, 2920. (c) Ding, H.; Li, Y.; Hu, H.; Sun, Y.; Wang, J.; Wang, C.; Wang, C.; Zhang, G.; Wang, B.; Xu, W.; Zhang, D. *Chem. - Eur. J.* **2014**, *20*, 14614. (d) Cai, S.-L.; Zhang, Y.-B.; Pun, A. B.; He, B.; Yang, J.; Toma, F. M.; Sharp, I. D.; Yaghi, O. M.; Fan, J.; Zheng, S.-R.; Zhang, W.-G.; Liu, Y. *Chem. Sci.* **2014**, *5*, 4693. (e) Calik, M.; Auras, F.; Salonen, L. M.; Bader, K.; Grill, I.; Handloser, M.; Medina, D. D.; Dogru, M.; Löbermann, F.; Trauner, D.; Hartschuh, A.; Bein, T. *J. Am. Chem. Soc.* **2014**, *136*, 17802. (f) Feldblyum, J. I.; McCreery, C. H.; Andrews, S. C.; Kurosawa, T.; Santos, E. J. G.; Duong, V.; Fang, L.; Ayzner, A. L.; Bao, Z. *Chem. Commun.* **2015**, *51*, 13894.

(7) (a) Waller, P. J.; Gándara, F.; Yaghi, O. M. *Acc. Chem. Res.* **2015**, *48*, 3053. (b) Ding, S.-Y.; Wang, W. *Chem. Soc. Rev.* **2013**, *42*, 548. (c) Bertrand, G. H. V.; Michaelis, V. K.; Ong, T.-C.; Griffin, R. G.; Dincă, M. *Proc. Natl. Acad. Sci. U. S. A.* **2013**, *110*, 4923. (d) Zhu, Y.; Wan, S.; Jin, Y.; Zhang, W. *J. Am. Chem. Soc.* **2015**, *137*, 13772.

(8) O'Keeffe, M.; Yaghi, O. M. *Chem. Rev.* **2012**, *112*, 675.

(9) (a) Chen, W.; Wang, J.-Y.; Chen, C.; Yue, Q.; Yuan, H.-M.; Chen, J.-S.; Wang, S.-N. *Inorg. Chem.* **2003**, *42*, 944. (b) Koh, K.; Wong-Foy, A. G.; Matzger, A. J. *Angew. Chem., Int. Ed.* **2008**, *47*, 677. (c) Koh, K.; Wong-Foy, A. G.; Matzger, A. J. *J. Am. Chem. Soc.* **2010**, *132*, 15005. (d) Doonan, C. J.; Morris, W.; Furukawa, H.; Yaghi, O. M. *J. Am. Chem. Soc.* **2009**, *131*, 9492. (e) Bunck, D. N.; Dichtel, W. R. *Chem. - Eur. J.* **2013**, *19*, 818.

(10) Zhou, T.-Y.; Xu, S.-Q.; Wen, Q.; Pang, Z.-F.; Zhao, X. *J. Am. Chem. Soc.* **2014**, *136*, 15885.

(11) Sing, K. S. W.; Everett, D. H.; Haul, R. A. W.; Moscou, L.; Pierotti, R. A.; Rouquérol, J.; Siemieniewska, T. *Pure Appl. Chem.* **1985**, *57*, 603.

DOI: 10.1021/jacs.6b01244
J. Am. Chem. Soc. 2016, 138, 4710−4713